INVESTIGATION OF THE EFFECT OF ANNEALING TEMPERATURE ON STRUCTURAL, OPTICAL AND ANTIBACTERIAL PROPERTIES OF COPPER OXIDE NANOPARTICLES PREPARED BY FACILE CO-PRECIPITATION ROUTE

H. ANWAR[a,*], S. M. B. NAQVI[a], B. ABBAS[a], M. SHAHID[b], M. IQBAL[a], M. SHAHARYAR[a], A. ISLAM[a], F. BATOOL[a], M. KHALID[a], A. JAMIL[a]
[a]*Department of Physics, University of Agriculture, Faisalabad-38040 Pakistan*
[b]*Department of Biochemistry, University of Agriculture, Faisalabad-38040 Pakistan*

Copper oxide (CuO) nanoparticles are important due to their excellent properties and applications such as nano electronics, gas sensors, solar cell and super conductors. Copper oxide have been successfully prepared by using co-precipitation method. $CuCl_2$. $2H_2O$ and NaOH are used in the synthesis of copper oxide nanoparticles as a precursers. Samples annealed at different temperatures such as 400 ºC, 500 ºC, 600 ºC and 700 ºC. The as prepared samples were investigated X-ray diffraction (XRD), scanning electron microscopy (SEM), UV-vis spectroscopy. Their using Antibacterial activity against the two bacterial strain Gram-positive and Gram negative such as (*E. coli* and *B. subtilis*) and Hemolysis. Was also investigated XRD analysis showed structure of copper oxide nanoparticles was monoclinic and average crystallite size was found to increase with an increase in annealing temperature in the range of 35 nm to 45 nm. Morphology of SEM images showed that CuO nanostructures were rod like at lower temperature but in higher temperature sphere- like shape was observed. UV-visible spectroscopy results revealed the variation of band gap energy with increasing annealing temperature. Samples prepared at higher temperatures exhibited high antibacterial activity for *E. coli* and *B. subtilis* and low toxicity. Low homolytic is safer to use in different applications.

(Received January 28, 2020; Accepted May 7, 2020)

Keywords: CuO nanoparticles, Annealing temperature, Antibacterial activity, Hemolysis

1. Introduction

Nanoparticles of metal oxides such as copper oxide have been present in many applications such as Nano electronics, solar energy, superconductors, gas sensors [1] and magnetic storage media [2]. In copper compounds, copper oxide is the simplest member of this family and show useful physical properties such as effect of electron correlation and high temperature superconductivity [3]. Many methods were introduced to prepare copper oxide nanoparticles with different size, shapes such as combustion method[4], sol gel [5-7], thermal oxidation [8] sono-chemical [9] and co-precipitate method [10] Mostly, precipitation method was used because of cost-effective approach, inexpensive, low temperature and energy [11]. Copper oxide is p-type semiconductor with narrow band gap of 1.2 eV to 1.8 eV. Copper oxide was synthesized with different nanostructure such as nanowire, nanoflower, nanoneedle and nanoparticles [12]. Copper oxide nanoparticles are robust, stable and have a longer life as compared to the agents of the antibacterial. Copper oxide also used in textiles and purification of water as effective materials. For lower concentration, copper oxide shows efficient results against the antibacterial activity. In the presence of air, copper oxide nanoparticles have fast oxidation for both physical and chemical instability [13]. The properties of antibacterial activity for the copper oxide are effective for growth reducing in many microorganism [14]. Some studies reported that copper oxide nanoparticles have been shown strong dependence of cytotoxic and copper oxide nanoparticles have been investigated previously for enhancing antibacterial properties [15]. The purpose of this

* Corresponding author: hafeez.anwar@gmail.com

study is to determine the behavior of CuO against the *E. coli* and *B. subtilis*. To realize the potential of copper oxide nanoparticles to act as an antibacterial agent [16-18] copper oxide nanoparticles with different shapes and sizes were synthesized by controlling the annealing temperature during the co-precipitation method. The prepared samples were analyzed by X-ray diffraction, Scanning electron microscopy and UV-vis spectroscopy. Furthermore, cytotoxic and antibacterial activity of these samples against to *E. Coli* and *B. Subtilis* was investigated.

2. Experimental

2.1. Chemicals and synthesis

All chemicals used throughout the research work were of analytical grade and purchased from sigma-Aldrich. The schematic diagram of preparation of copper oxide nanoparticles is shown in Fig 1. The CuO nanoparticles were synthesized by co-precipitation method using copper chloride $CuCl_2$. $2H_2O$ and sodium hydroxide (NaOH) as precursors. Aqueous solution of copper chloride and NaOH (1;2) M were prepared. Sodium hydroxide solution was added dropwise in the solution. The reaction was proceeded for 3 h after the complete addition of sodium hydroxide solution and it was kept overnight. Obtained precipitation was filtered and washed three times with ethanol to remove the byproducts. The moisture free content was obtained after drying at 80 ℃ for 2 h in an oven Model (Shel-Lab). Then the grinded samples were annealed at different temperatures such as 400 ºC, 500 ºC, 600 ºC and 700 ºC for 2 h in furnace Model (SNOL-LHM) and labelled as S1, S2, S3, S4 and S5.

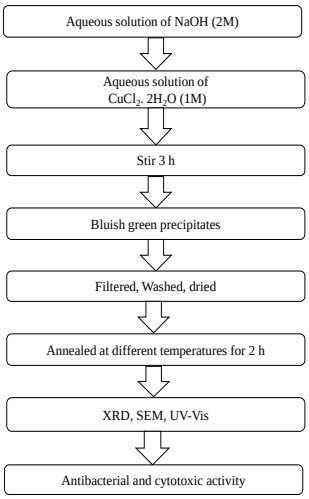

Fig. 1. Preparation procedure of CuO nanoparticles.

2.2. Characterization

The powder X-ray diffraction was performed through XRD system Model PANalytical with Nickel filtere CuK_α (λ = 1.50405 Å) radiation. The particle size was calculated from broadening of line using Scherer's formula. The scanning electron microscope (SEM) studies were performed using SEM Model (JEOL- JSM 5910) to study the morphology of the prepared nanoparticles. The absorption spectra of samples were recorded with UV-Vis spectrophotometer PG (Model T-80). The spectra were recorded in the range of (200-800 nm). The average crystallite size (Scherrer's equation), lattice parameter, volume of unit cell and X-ray density were measured by using the following relations

$$D = \frac{0.9\lambda}{B\cos\theta} \quad (1)$$

$$\frac{1}{d^2} = \frac{1}{sin^2\,\beta}\left(\frac{h^2}{a^2} + \frac{k^2\,sin^2\beta}{b^2} + \frac{l^2}{c^2} - \frac{2hlcos\beta}{ac}\right) \quad (2)$$

$$V_{cell} = \text{abcsin}\beta \quad (3)$$

$$\text{D} = \frac{ZM}{N_{AV_{Cell}}} \quad (4)$$

where D is the size of crystal, B is the line width (FWHM), θ is the diffraction angle and the λ is the wavelength of X-ray radiation. Z is the number of atoms per unit cell, M is the molar weight of the copper oxide, N_A is Avogadro number and V_{cell} is the volume of the unit cell.

2.3. Antibacterial activity of copper oxide nanoparticles

For the antibacterial activity of CuO nanoparticles (0.05 g) were prepared in dimethyl sulfoxide at the concentration of 1 µL. Antibacterial activities of copper oxide nanoparticles were determined with the help of well diffusion method [19]. Antibacterial activity of CuO nanoparticles prepared at different temperatures was tested against the *E. coli* and *B. subtilis.* Nutrient ager (Oxide, UK) was used for growth of bacterial strain in Petri-dishes. The test samples were loaded (50 µL) in the well. The Petri-plates of *E. coli* and *B. subtilis* were incubated at 37 ºC for 24 h in incubator (Memmert, Germany). The zone of inhibition was recorded of each CuO nanoparticles sample in the mili-meter.

2.4. Hemolysis Activity of copper oxide nanoparticles

The cytotoxic activity was determined by method used previously studies [20]. Blood (5mL) were collected from the healthy volunteer in containing heparinized tube. The blood was centrifuged at 1500 rpm for 3 minutes. Plasma was discarded and the pellet was washed three times with sterile phosphate buffer saline (PBS). A volume of 0.5 of mL the cell suspension was mixed with 0.5mL of the samples. The mixture was centrifuged for 5 min. The free hemoglobin in the supernatant was measured in microplate reader (BioTek, USA) at 540 nm. PBS was used as negative control and Triton-X-100 as positive control for this assay. The level of percentage hemolysis by the samples was calculated according to the following formula:

$$\textbf{\% Cytotoxic} = \frac{\mathbf{100} \times (\boldsymbol{sample\ absorbance - negative\ control\ absorbance})}{\boldsymbol{Postive\ control\ absorbance}} \quad (5)$$

3. Results and discussion

3.1. Structural analysis

The XRD patterns of prepared CuO nanoparticles at different temperatures (400 ºC, 500 ºC, 600 ºC and 700 ºC) and untreated are shown in Fig 2. X-ray diffraction patterns confirm of monoclinic structure of copper oxide nanoparticles. The observed diffraction peaks at 2θ of 32.75º, 35.35º, 38.74º, 48.9º, 53.86º, 58.29º, 61.42º, 66.36º, 68.18º, 72.36º, 75.23º referred to hkl planes (110), (-111), (111), (-112), (020), (202), (-113), (022), (220), (311), (004) respectively. The JCPDS file no. 36-1451 revealed that the synthesized copper oxide has the monoclinic structure. XRD investigation confirmed that the average crystallite size increased by increasing the annealing temperature. The lattice parameters, volume of unit cell and X-ray density were also measured from X-ray diffraction data and obtained results are listed in Table 1.

The average crystallite size is calculated by Scherrer's formula Eq. 1 it is increased from 35 to 48 nm with the increase in annealing temperatures. The untreated sample has crystallite size 24 nm. Therefore, it is found that the growth of copper oxide gradually increased with increase in heat treatment and maximizes the crystallite size 48 nm at the temperatures 700 ºC (Fig. 3).

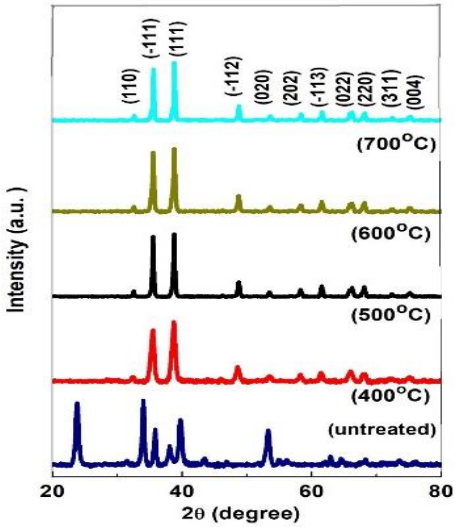

Fig. 2. XRD pattern of CuO prepared at different temperature.

Table 1. Structural parameters of prepared CuO nanoparticles from XRD.

Sr. No.	Sample	Average Crystallite size (nm)	Lattice parameters (Å)			Volume $(Å)^3$	Density (g/cm^3)
			a	b	c		
1	S1 (untreated)	24	0.4797	0.3432	0.5344	86.76	6.089
2	S2 (400 ℃)	35	0.4713	0.3961	0.5123	94.31	5.602
3	S3 (500 ℃)	36	0.4709	0.3422	0.5118	81.32	6.497
4	S4 (600 ℃)	38	0.4711	0.3423	0.5118	81.38	6.493
5	S5 (700 ℃)	48	0.4704	0.3407	0.5114	80.82	6.539

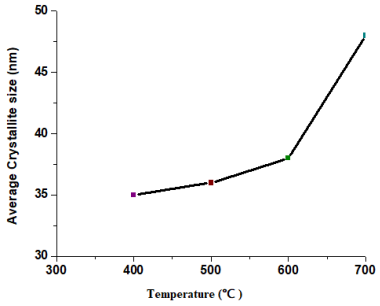

Fig. 3. The variation of crystallite size with different temperature.

3.2. SEM analysis

Scanning microscopy revealed the information about surface morphology and composition of nanostructure. The scanning electron microscopy (SEM) images of untreated sample of nanoparticles is shown in Fig. 4a. The morphology of SEM image shows that copper oxide nanostructures are rod like (Fig. 4b) at lower annealing temperature than agglomerate and form sphere-like shape at higher temperature (Fig. 4c). Annealing temperature has significant effect on morphology of nanostructures.

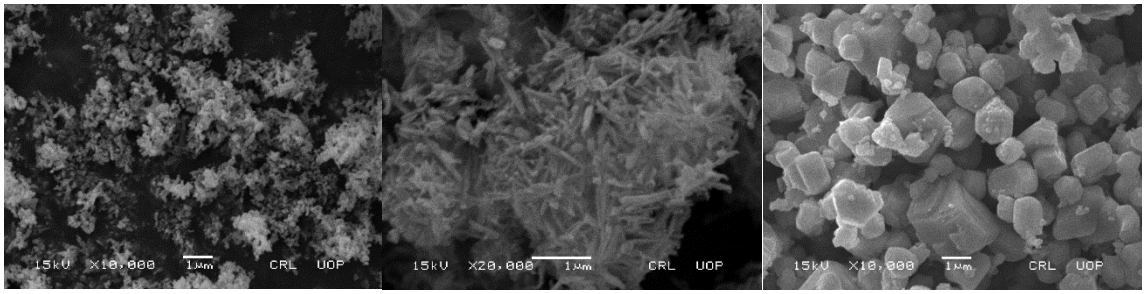

(a) *(b)* *(c)*

Fig. 4. SEM images of CuO nanoparticles (a) untreated (b) annealed at 500 ºC (c) annealed at 700 ºC..

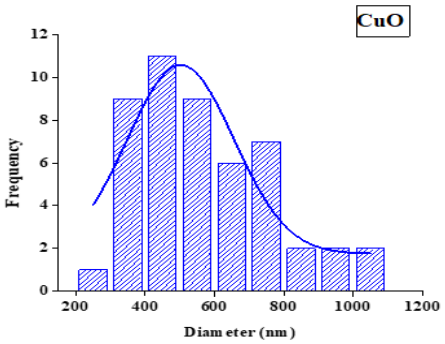

Fig. 5. The particle size distribution of CuO-NPs of Sample of S5(700 ºC).

3.3. UV-vis analysis

The absorption spectra of copper oxide nanoparticles synthesized by the co-precipitation method at different temperatures are shown in Fig 5. The sample S5 have maximum absorption peat at 350 nm.

Energy band gap of copper oxide nanoparticles (sample S5) was calculated using the following formula;

$$(\alpha h\nu) = A\,(h\nu - E_g)^n \tag{6}$$

where the E_g is the energy band gap of the material, ν is the frequency of the incident radiation, α is the co-efficient of the absorption in the cm^{-1}, h is the plank's constant, A is the transition matrix, n is the coefficient depending on the nature of transition. Absorption coefficient is obtained using the relation given below,

$$\alpha.d = \ln(1/T) \tag{7}$$

where T is transmittance which is calculated by the Beer- Lambert law,

$$B = \log10(T) \tag{8}$$

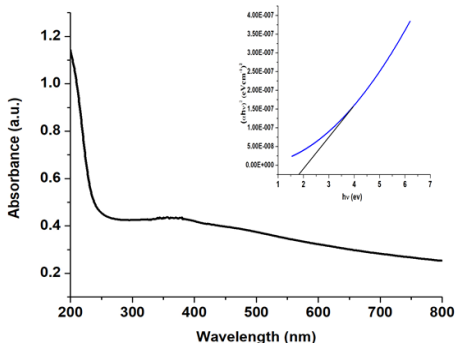

Fig. 5. UV-vis spectrum of sample S5. Inset: plot $(\alpha h\nu)^2$ vs hv.

where d is the path length of the wave in 1cm. To find the band gap of the copper oxide graph of $(\alpha h\nu)^2$ against the energy hν was plotted. The value of energy band gap Eg where the line intersects with the hν as shown in Fig. 5.

The obtained value of the direct energy band gap of copper oxide nanoparticles is 1.7 eV and it is accordance with the previous by reported work [21].

3.3. Antibacterial activity of copper oxide nanoparticles

Antibacterial activities of copper oxide nanoparticles were analyzed against Gram positive (*B. subtilis*) and Gram-negative (*E. coli*) bacterial strain. The copper oxide nanoparticles showed significance antibacterial activity against selected bacteria. The smallest copper oxide nanoparticles processing the particle size 24 nm (untreated) were recorded as 22 mm against *E. coli* and 17mm against *B. subtilis.* Therefore, copper oxide nanoparticles at higher temperature is increased than the zone of inhibition is increased in the *E. coli* bacterial strain but in *B. subtilis* bacterial strain the zone of inhibition increased then slightly decreased as shown in Table 2.

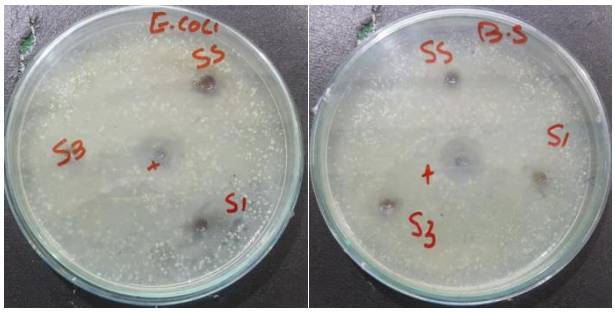

Fig. 6. Zone of inhibition of copper oxide against the E. coli and B. subtilis numbers (S1, S3, S5) at different temperature (untreated, 400 ℃, 700 ℃).

Table 2. zone of inhibition of copper oxide at different temperatures against the E. coli and B. subtilis bacterial strain.

Sample	*E. coli* (mm)	*B. subtilis* (mm)
CuO (untreated)	22	17
CuO (400℃)	23	20
CuO (700℃)	27	21
Ampicillin	29	24

3.4. Hemolysis activity of copper oxide nanoparticles

This rapid assay is used to screen the cytotoxicity of different samples. The percentage of hemolysis S1(untreated), S2 (500 ºC) and S3(700 ºC) was shown in Fig. 7. The hemolysis activity

was measured in S1(untreated) of 13.81% and less hemolytic activity 8. 62% was measured in S5 (700 ºC).

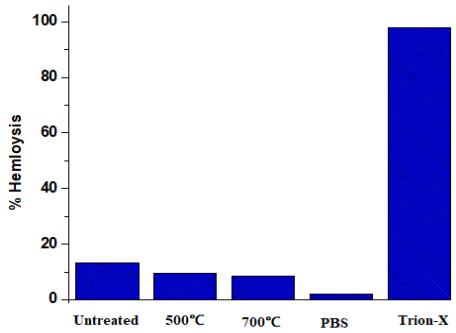

Fig. 7. Hemolysis of copper oxide nanoparticles at different temperature.

4. Conclusions

Copper oxide nanoparticles has been synthesized using co-precipitation method and annealed for different temperatures. Their X-ray diffraction analysis has confirmed monoclinic type structure. The average crystallite size was found in the range of 35 to 48 nm. The morphology of the copper oxide shows uniform distribution of grains and morphology transformation from rod like to sphere like structure. The synthesized copper oxide nanoparticles exhibited an effective antibacterial potential and prevented the growth of *E.Coli* and *B. Subtilis*. Low hemolytic safer to use in different applications.

Acknowledgments

Author's acknowledged the financial assistant provide by Pakistan Science Foundation under project No; PSF-NSF/Eng/P-UAF(05).

References

[1] M. Salavati-Niasari, F. Davar, Materials Letters **441**, 443 (2009).
[2] J. F. Xu, W. Ji, Z. X. Shen, S. H. Tang, Solid State Chemistry **516**, 519 (1999).
[3] H. Elshamy, Applied Surface Science **2997**, 3001 (2013).
[4] M. Frietsch, F. Zudock, J. Goschnick, M. Bruns, Sensors and Actuators **379**, 381 (2000)
[5] P. Mallick, S. Sahu, Nanoscience and Nanotechnology **71**, 74 (2012).
[6] M. Fu, Y. Li, P. Lu, J. Liu, F. Dong, Applied Surface Science **1587**, 1591 (2011).
[7] Z. N. Kayani, M. Umer, S. Riaz, Electronic material **3704**, 3709 (2015).
[8] M. Kaur, K. P. Muthe, S. K. Despande, S. Choudhury, J. B. Singh, Crystal Growth **670**, 675 (2006).
[9] N. Wongpisutpaisan, P. Charoonsuk. (2011), Energy Procedia **404**, 409 (2011).
[10] K. Phiwdang, S. Suphankij, W. Mekprasart, Energy procedia **740**, 745 (2013).
[11] C. L. Carnes, K. J. Klabunde, Molealar catalysis A: chemical **227**, 236 (2003).
[12] R. V. Kumar, Y. Diamant, A. Gedanken, Chem. Mater **2301**,2305 (2000).
[13] D. Das, B. Chandra, P. Phukon, S. Kumar, Colloids and Surfaces B: Biointerfaces **430**, 433 (2013).
[14] H. J. Lee, S. Y. Yeo, S. H. Jeong, Materials science **2199**, 2204 (2003).
[15] C. Lok, C. Ho, R. Chen, Q. He, W. Yu, H. Sun, C. Che, Proteome Research **916**, 924 (2006).
[16] R. S. Society, E. Hassan, S. City, SMU Medical **91**, 101 (2014).

[17] A. A. Alswat, M. Bin, A. Saleh, Antibacterial Activities **19**, 24 (2017).
[18] J. P. Ruparelia, A. Kumar, S. P. Duttagupta, Acta Biomaterials **707**, 716 (2008).
[19] M. Raffi, S. Mehrwan, Annals of Microbology **75**, 80 (2010).
[20] A. M. Studer, L. K. Limbach, L. Van Duc, F. Krumeich, E. K. Athanassiou, L. C. Gerber, W. J. Stark, Toxicology Letters **169**, 174 (2010).
[21] D. S. Murali, S. Kumar, R. J. Choudhary, A. D. Wadikar, M. K. Jain, A. Subrahmanyam, AIP Advances **1**, 6 (2015).